Journal of Thermal Analysis and Calorimetry, Vol. 88 (2007) 1, 37–41

FORMATION AND PROPERTIES OF THE $Fe_8V_{10}W_{16-x}Mo_xO_{85}$ TYPE SOLID SOLUTION

P. Tabero[*]

Department of Inorganic and Analytical Chemistry, Szczecin University of Technology, Al. Piastów 42 , 71-065 Szczecin, Poland

Solid solution phases of a formula $Fe_8V_{10}W_{16-x}Mo_xO_{85}$ where $0<x\leq4$, have been obtained, possessing a structure of the compound $Fe_8V_{10}W_{16}O_{85}$. It was found on the base of XRD and DTA investigations that these solution phases melted incongruently, with increasing the value of x, in the temperature range from 1108 (x=0) to 1083 K (x=4) depositing Fe_2WO_6 and WO_3. The increase of the Mo^{6+} ions content in the crystal lattice of $Fe_8V_{10}W_{16}O_{85}$ causes the lattice parameters a=b contraction with c being almost constant. IR spectra of the $Fe_8V_{10}W_{16-x}Mo_xO_{85}$ solid solution phases have been recorded.

Keywords: *DTA, $Fe_8V_{10}W_{16-x}Mo_xO_{85}$ solid solution phases, IR, XRD*

Introduction

The literature survey has shown, that in the Fe_2O_3–V_2O_5–WO_3 system the phase of general formula $Fe_8V_{10}W_{16}O_{85}$ is formed [1–3]. It crystallizes in a tetragonal system, and its unit cell parameters are as follows: a=b=1.9753 nm, c=0.3717 nm. This compound is known to melt at 1103 K with depositing two solid products, i.e. Fe_2WO_6 and WO_3. Besides, a solid solution of V_2O_5 in Fe_2WO_6 has been found to occur in the three-component system [4]. On the other hand, in the Fe_2O_3–V_2O_5–MoO_3 system $FeVMoO_7$, $Fe_4V_2Mo_3O_{20}$ phases as well as a solid solution of MoO_3 in $Fe_2V_4O_{13}$, are formed [5–9]. $FeVMoO_7$ crystallizes in a triclinic system and melts incongruently at 953 K with the deposition of $Fe_4V_2Mo_3O_{20}$ as a solid product. The compound $Fe_4V_2Mo_3O_{20}$ crystallizes in a tetragonal system, and melts incongruently at 1033 K with depositing two solid products, i.e. $Fe_2(MoO_4)_3$ and Fe_2O_3. The equal charge and approximate values of Mo^{6+} and W^{6+} ionic radii let one expect the formation of solid solutions as a result of a substitution of molybdenum for tungsten and tungsten for molybdenum in the quaternary Fe_2O_3–V_2O_5–WO_3–MoO_3 system. The literature scan has shown, however that despite these similarities (in charge and ionic radii) there are considerable differences in the physico-chemical properties of Mo^{6+} and W^{6+} ions affecting the crystal structure of the forming phases. Numerous polymorphic modifications of WO_3 stable at different temperatures are built up from highly distorted corner-shared octahedra forming the framework analogous to this of ReO_3 [10]. On the other hand, the crystal lattice of the orthorhombic modification of MoO_3, which is stable to its melting point at 1068 K, is built up from corner and edge-shared highly distorted octahedral which leads to the formation of the unique layered structure [10]. The solubility of WO_3 in orthorhombic MoO_3, as well as MoO_3 in monoclinic WO_3 is limited and does not exceed 3 mol% [11]. Besides, in the WO_3–MoO_3 system several phases of the $W_{1-x}Mo_xO_3$ type differing in composition are formed but always adopting a more or less distorted ReO_3 type structure [12]. The phase relations in the V_2O_5–MoO_3 and V_2O_5–WO_3 systems are the next examples of differences in properties of Mo^{6+} and W^{6+} ions. In the V_2O_5–MoO_3 system [13–16] the $V_9Mo_6O_{40}$ compound as well as the solid solution of the $V_{2-x}Mo_xO_5$ type exist with $0<x<0.3$, whereas in the case of the V_2O_5–WO_3 system only solid solution of the $V_{2-x}W_xO_5$ type with a $x<0.07$ or $x<0.15$ solubility limit is formed [17, 18]. Also in the case of Fe_2O_3–MoO_3 and Fe_2O_3–WO_3 systems differences can be found. It follows from the literature survey that in the Fe_2O_3–MoO_3 system one compound, $Fe_2(MoO_4)_3$ exists, built up from MoO_4 tetrahedra and FeO_6 octahedra [19]. On the other hand, in the case of Fe_2O_3–WO_3 system the solid state synthesis leads to the formation of the Fe_2WO_6 compound, melting at 1373 K, in the crystal structure of which both iron and tungsten ions occupy sites in the octahedral environment [1–3, 20, 21]. By using the solution method, one can obtaine the $Fe_2(WO_4)$ phase, isotypical with $Fe_2(MoO_4)$, which decomposes in the solid-state at above 600°C to Fe_2WO_6 and WO_3 [22]. The all above mentioned facts make the investigation into the substitution of molybdenum for tungsten in the case of the Fe_2O_3–V_2O_5–WO_3–MoO_3 system very interest-

* ptab@ps.pl

1388–6150/$20.00

Akadémiai Kiadó, Budapest, Hungary
Springer, Dordrecht, The Netherlands

ing. This paper, the first from the planned group, shows the results of works connected with the substitution of molybdenum for tungsten in the case of the $Fe_8V_{10}W_{16}O_{85}$ compound.

Experimental

The following reagents were used for the research: α-Fe_2O_3, p.a. (POCh, Poland), V_2O_5, p.a. (POCh, Poland), WO_3, p.a., (Fluka AG, Switzerland) and a pure MoO_3 (POCh, Poland).

For the experiments 7 samples were selected with contents corresponding to $Fe_8V_{10}W_{16-x}Mo_xO_{85}$ formula with x=0, 2, 4, 6, 8, 12 and 16. They represented the whole component concentration range of the system: $Fe_8V_{10}W_{16}O_{85}$ – hypothetical $Fe_8V_{10}Mo_{16}O_{85}$ (not existing). The content of V_2O_5 and Fe_2O_3 in the mixtures was always constant and amounted to 20.00 and 16.00 mol%, respectively. The composition of the samples prepared for investigations is listed in Table 1.

The samples were synthesized from oxides. Weighed in suitable proportions preparations were homogenized and calcinated at 873, 923, 973, 1023 and 1053 K in 24 h cycles. After each heating cycle the samples were triturated and examined with the help of XRD. The equilibrium state was confirmed by comparing the results of two consecutive heating cycles. The results being identical, the equilibrium state was considered to be established. The samples obtained after the last heating cycle were additionally examined by the DTA and IR methods. Results of investigations by XRD, DTA and IR methods allow a determination of composition of samples and establishing of their melting temperatures [23–27].

The examination by the method of differential thermal analysis (DTA) was performed using an apparatus of Paulik–Paulik–Erdey type, (MOM, Hungary). Samples of 500 mg were investigated in air up to the temperature of 1273 K in quartz crucibles at a heating rate of 10 K min^{-1}.

The contents of the obtained preparations were determined on the base of their powder diffraction patterns measured by the DRON-3 diffractometer, a product of Bourevestnik, Sankt Petersburg (Russia), applying the radiation CoK_α/Fe. The identification of the individual phases was performed on the ground of the PDF cards [28] and the literature data [1–22].

The IR measurements were made using a Specord M 80 spectrometer (Carl Zeiss, Jena Germany). The IR spectra were taken using the halide disc technique. The samples were mixed with KBr in a mass ratio of 1:300 and then pressed to pellets. The measurements were made in the wavenumber region of 1500–200 cm^{-1}.

Results and discussion

The composition of the samples obtained after the last heating stage, that means – having reached the equilibrium state, is presented in Table 1.

The analysis of diffraction patterns recorded at subsequent stages of synthesis showed that, with the exclusion of the sample for which x=16, only after the calcinations at 923 K, the diffractograms revealed, beside the reflections due to initial oxides, also some new reflections, characteristic of the $Fe_8V_{10}W_{16}O_{85}$ type phase. After the succeeding calcinations stages their intensity increased significantly, which was accompanied by a distinct decrease in the intensity of the reflections characteristic of Fe_2O_3, V_2O_5, MoO_3 and WO_3.

Powder diffraction patterns of the preparations 1–3 (Table 1), where $x\in$ <0;4>, after the last calcination cycle at 1053 K, were similar to one another and to the diffractogram of $Fe_8V_{10}W_{16}O_{85}$, both with respect to the number and to the mutual intensity relations of the recorded diffraction lines. The angular positions of these lines were shifted with increasing the MoO_3 content in initial oxide mixtures towards higher angles 2θ, in comparison with the diffractogram of pure $Fe_8V_{10}W_{16}O_{85}$, i.e. they corresponded to

Table 1 The composition of the initial oxide mixtures (x/mol%) and the results of XRD analysis of the samples of the $Fe_8V_{10}W_{16-x}Mo_xO_{85}$ type general formula after the last heating cycle

No.	The composition of the initial mixtures of the $Fe_8V_{10}W_{16-x}Mo_xO_{85}$ type phases					Phase detected after the last heating cycle
	x	Fe_2O_3/mol%	V_2O_5/mol%	WO_3/mol%	MoO_3/mol%	
1	0	16	20	64	0	$Fe_8V_{10}W_{16}O_{85}$
2	2	16	20	56	8	$Fe_8V_{10}W_{14}Mo_2O_{85}$
3	4	16	20	48	16	$Fe_8V_{10}W_{12}Mo_4O_{85}$
4	6	16	20	40	24	$Fe_8V_{10}W_{12}Mo_4O_{85}$, $Fe_2(MoO_4)_3$, $V_9Mo_{6-x}W_xO_{40}$
5	8	16	20	32	32	$Fe_8V_{10}W_{12}Mo_4O_{85}$, $Fe_2(MoO_4)_3$, $V_9Mo_{6-x}W_xO_{40}$
6	12	16	20	24	40	$Fe_2(MoO_4)_3$, $V_9Mo_{6-x}W_xO_{40}$
7	16	16	20	0	64	$Fe_2(MoO_4)_3$, $V_9Mo_{6-x}W_xO_{40}$, $V_{2-x}M_xO_5$

smaller interplanar distances *d*. The obtained results indicated that a substitutional solid solution of a general formula $Fe_8V_{10}W_{16-x}Mo_xO_{85}$ is formed by an incorporation of the Mo^{6+} ions into the crystal lattice of $Fe_8V_{10}W_{16}O_{85}$ instead of W^{6+}. The formulae of obtained solid solution were evaluated from the content of initial oxides. The maximal solubility of MoO_3 in $Fe_8V_{10}W_{16}O_{85}$ at an ambient temperature is equal to 16 mol% in terms of the oxides contents. It corresponds to a replacement of 25 mol% of W^{6+} ions in the crystal lattice of $Fe_8V_{10}W_{16}O_{85}$ by Mo^{6+} ions – the fact confirming the $Fe_8V_{10}W_{12}Mo_4O_{85}$ formula (Table 1, sample 3).

Phase analysis of the samples for which x=6 and x=8 (Table 1, samples 4 and 5) showed that they contained beside the solid solution $Fe_8V_{10}W_{12}Mo_4O_{85}$, i.e. the one with maximal extent of Mo^{6+} incorporation into the structure of $Fe_8V_{10}W_{16}O_{85}$, also $Fe_2(MoO_4)_3$ and $V_9Mo_6O_{40}$. The angular positions of the diffraction lines characteristic of $V_9Mo_6O_{40}$ was shifted towards higher or lower angles 2θ, in comparison with the diffractogram of pure $V_9Mo_6O_{40}$, which is typical of solid solutions of MoO_3 and WO_3 in V_2O_5 [13–18]. It means that in this case a solid solution of the $V_9Mo_{6-x}W_xO_{40}$ type is formed. In subsequent preparation, for which x=12 (Table 1, sample 6), the intensity of the diffraction reflections of $Fe_8V_{10}W_{16-x}Mo_xO_{85}$ type solid solution was increasing until the calcination stage at 973 K. The intensity of these lines was however relatively low indicating low content of this phase in the reaction mixture. This diffraction pattern contained the reflections characteristic of the $V_9Mo_{6-x}W_xO_{40}$ type solid solution and $Fe_2(MoO_4)_3$, as well. After the succeeding calcination stage at 1023 K the reflections characteristic of the $Fe_8V_{10}W_{16-x}Mo_xO_{85}$ type solid solution disappeared. Phase analysis of this sample showed that it contained beside $V_9Mo_{6-x}W_xO_{40}$ type solid solution also $Fe_2(MoO_4)_3$. The last heating stage at 1053 K did not change the phase composition in this preparation. On the other hand, the diffraction patterns of the preparation for which x=16 (Table 1, sample 7), i.e. hypothetical $Fe_8V_{10}Mo_{16}O_{85}$, recorded after any heating stage, did not contain the reflections characteristic of the $Fe_8V_{10}W_{16}O_{85}$ type phase. Phase analysis of this sample after the last heating cycle at 1053 K showed that beside $Fe_2(MoO_4)_3$ it contained solid solutions of the $V_9Mo_{6-x}W_xO_{40}$ and $V_{2-x}M_xO_5$ type, where M=Mo,W. It indicates that tungsten is an essential ingredient in the process of the $Fe_8V_{10}W_{16}O_{85}$ type phases formation. Moreover, taking the $Fe_8V_{10}W_{12}Mo_4O_{85}$ formula into consideration, i.e. the one with maximal extent of Mo^{6+} incorporation into the structure of $Fe_8V_{10}W_{16}O_{85}$, to preserve this structure, no more than 25 mol% of molybdenum ions can be substituted for the tungsten ones.

In the further part of the research, powder diffraction patterns of monophase samples of the obtained $Fe_8V_{10}W_{16-x}Mo_xO_{85}$ type solid solution were indexed (program Refinement) and the calculated unit cell parameters and unit cell volumes are presented in Table 2. An analysis of the data compiled in Table 2 allows to confirm the conclusion that the $Fe_8V_{10}W_{16-x}Mo_xO_{85}$ type solid solution with the structure of $Fe_8V_{10}W_{16}O_{85}$ is formed. With increasing the incorporation extent of the smaller Mo^{6+} ions into the $Fe_8V_{10}W_{16}O_{85}$ structure, the unit cell parameters a=b are shortened whereas parameter c being almost constant.

The obtained monophase preparations after the last heating cycle, i.e. containing only the solid solution $Fe_8V_{10}W_{16-x}Mo_xO_{85}$ (Table 1, samples 1–3) were subjected to the DTA investigation. In the DTA curves of these samples two endothermic effects were recorded up to 1273 K. The beginning temperature of the first distinctly pronounced effect decreased with increasing x in the phases $Fe_8V_{10}W_{16-x}Mo_xO_{85}$ from 1108 K for the sample where x=0 to 1083 K for the sample where x=4. The second effect recorded in the DTA curves of the monophase preparations began at 1213 K for x=0, and its onset temperature, decreasing for the subsequent samples with increasing x, amounted to 1183 K for x=4. The second effect was always much smaller than the first one and it was registered as a poorly pronounced remnant effect.

In order to explain the nature of these endothermic effects and first of all to establish the way of melting the solid solution $Fe_8V_{10}W_{16-x}Mo_xO_{85}$, the samples for which x=0, 2 and 4 were additionally heated for 3 h at 1143 K, i.e. at temperature close to the extremum temperatures of the first endothermic effect registered in the DTA curves of these preparations. After heating these samples they were cooled rapidly to ambient temperature. Phase analysis of the preparations partially melted at this temperature showed that they comprised a mixture of WO_3, Fe_2WO_6 and solid solutions of $V_9Mo_{6-x}W_xO_{40}$ and $V_{2-x}M_xO_5$ type. Taking into account that both $V_9Mo_6O_{40}$ and V_2O_5 at the temperatures the heating of samples was conducted at do not exist already as solid phases [13–18], so they crystallize from the liquid, it was concluded that the

Table 2 Unit cell parameters and volumes for the $Fe_8V_{10}W_{16}O_{85}$ [3] and the solid solution $Fe_8V_{10}W_{16-x}Mo_xO_{85}$ type phases

x	Formula	a=b/nm	c/nm	V/nm^3
0	$Fe_8V_{10}W_{16}O_{85}$	1.9753(3)	0.3717(2)	1.4503
2	$Fe_8V_{10}W_{14}Mo_2O_{85}$	1.9733(8)	0.3716(4)	1.4468
4	$Fe_8V_{10}W_{12}Mo_4O_{85}$	1.9725(6)	0.3713(5)	1.4446

investigated solid solution $Fe_8V_{10}W_{16-x}Mo_xO_{85}$ melt incongruently and their solid products of melting are the WO_3 and Fe_2WO_6.

The pure phase $Fe_8V_{10}W_{16}O_{85}$ as well as the solution phases $Fe_8V_{10}W_{16-x}Mo_xO_{85}$ were also subjected to an investigation with the use of infrared spectroscopy (IR).

Figure 1 shows the IR spectra of γ-Fe_2WO_6 (curve a), $Fe_8V_{10}W_{12}Mo_4O_{85}$ (curve b) $Fe_8V_{10}W_{16}O_{85}$ (curve c), $FeVO_4$ (curve d) and monoclinic modification of WO_3 (curve e). The IR spectra of γ-Fe_2WO_6 (curve a) and WO_3 (curve e) differ distinctly from the remaining spectra of the phases $Fe_8V_{10}W_{12}Mo_4O_{85}$ (curve b), $Fe_8V_{10}W_{16}O_{85}$ (curve c) and $FeVO_4$ (curve d) that are very similar to one another. In the case of the solid solution $Fe_8V_{10}W_{12}Mo_4O_{85}$ an evident broadening of the absorption bands corresponding respectively to each other is observed in comparison to the IR spectrum of $Fe_8V_{10}W_{16}O_{85}$. This is undoubtedly due to an appearance of numerous additional Mo–O bonds in the structure of $Fe_8V_{10}W_{12}Mo_4O_{85}$.

The IR spectrum of the $Fe_8V_{10}W_{16}O_{85}$ reveals the presence of absorption bands with their maxima at 922, 654, 486, 368 and 320 cm^{-1} [2, 3]. With increasing the incorporation extent of the lighter Mo^{6+} ions into the structure of $Fe_8V_{10}W_{16}O_{85}$ a relatively small shift of the respective absorption bands towards lower wavenumbers is observed. Their maxima at 912, 640, 480, 366 and 320 cm^{-1} are not so distinctly pronounced as in the case of $Fe_8V_{10}W_{16}O_{85}$ spectrum. A broad absorption band lying at the range of wavenumbers 1050–800 cm^{-1} with a maximum at 912 cm^{-1} in the IR spectrum of $Fe_8V_{10}W_{12}Mo_4O_{85}$ phase can be attributed to stretching vibrations of V–O bonds in VO_4 tetrahedra [2, 3, 29–31]. It is noteworthy that broad absorption band in the IR spectrum of WO_3 (curve e) covering the wavenumber region of 1000–700 cm^{-1} is caused by stretching vibrations of W–O bonds in highly distorted WO_6 octahedra. Thus, the absorption band covering the wavenumber region of 1050–800 cm^{-1} in the IR spectrum of the $Fe_8V_{10}W_{12}Mo_4O_{85}$ phase can be attributed to stretching vibrations of the W–O and Mo–O bonds in the MO_6 octahedra, as well. Another very broad absorption band covering the wavenumber region of 800–540 cm^{-1} with a 640 maximum can correspond also to stretching vibrations of WO_6 and MoO_6 octahedra. A similar absorption band with a 640 cm^{-1} maximum was noticed in an IR spectrum of γ-Fe_2WO_6 phase, comprising WO_6 and FeO_6 octahedra in its structure [20] (curve a). In this wavenumber range absorption bands can also occur corresponding to stretching vibrations of Fe–O bonds in FeO_5 polyhedra, which was observed in IR spectrum of $FeVO_4$ [29]. Another absorption band recorded in the range of 540–400 cm^{-1} can be the most likely ascribed to stretching vibrations of Fe–O bonds in FeO_6 octahedra [29–31]. A similar absorption bands were noticed in the IR spectra of γ-Fe_2WO_6 and $FeVO_4$ in the structure of which the FeO_6 octahedra occur. On the other hand, bands lying within the wavenumber range of 400–250 cm^{-1} may correspond to bending vibrations of M–O bonds in VO_4 tetrahedra and WO_6 octahedra or be of a mixed character [29–31]. Analysis of the IR specta of the $Fe_8V_{10}W_{16-x}Mo_xO_{85}$ type phases permits assumption that these phases are built up from VO_4 tetrahedra as well as WO_6 and FeO_6 octahedra. One cannot also preclude occurrence of FeO_5 polyhedra in the crystal lattice.

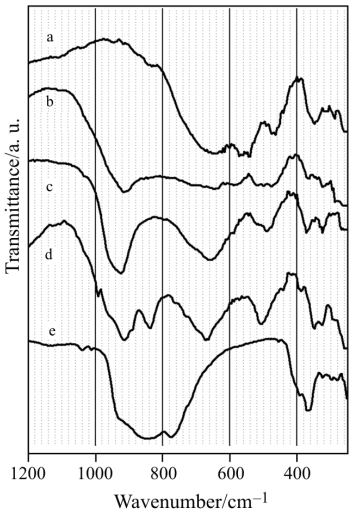

Fig. 1 IR spectra of a – γ-Fe_2WO_6, b – $Fe_8V_{10}W_{12}Mo_4O_{85}$, c – $Fe_8V_{10}W_{16}O_{85}$, d – $FeVO_4$ and e – monoclinic modification of WO_3

Conclusions

- The solid solutions of $Fe_8V_{10}W_{16-x}Mo_xO_{85}$ type, possessing the structure of $Fe_8V_{10}W_{16}O_{85}$ are formed in the quaternary system Fe_2O_3–V_2O_5–WO_3–MoO_3. The maximal solubility of MoO_3 at an ambient temperature amounts to 16 mol%, x=4.
- With the increase of x a decrease of the a=b parameters of the unite cell occurs, with c parameter being almost constant.
- The $Fe_8V_{10}W_{16-x}Mo_xO_{85}$ solid solutions melt incongruently. Their melting temperature decreases with increasing the content of MoO_3 and changes from being equal to 1108 K for x=0 down to 1083 K for x=4.
- The solid products of incongruent melting the $Fe_8V_{10}W_{16-x}Mo_xO_{85}$ solid solutions are the Fe_2WO_6 and WO_3.
- Analysis of the IR spectra of the $Fe_8V_{10}W_{16-x}Mo_xO_{85}$ type phases permits assumption that these phases are built up from VO_4, WO_6, FeO_6 and FeO_5 polyhedra.

References

1 J. Walczak and I. Rychlowska-Himmel, J. Mater. Sci., 2929 (1994) 2745.
2 J. Walczak, I. Rychlowska-Himmel and P. Tabero, J. Therm. Anal. Cal., 56 (1999) 419.
3 I. Rychlowska-Himmel and P. Tabero, J. Therm. Anal. Cal., 65 (2001) 537.
4 J. Walczak and I. Rychlowska-Himmel, Thermochim. Acta, 239 (1994) 269.
5 J. Walczak, J. Ziolkowski, M. Kurzawa and L. Trzesniowska, Pol. J. Chem., 59 (1985) 713.
6 J. Walczak and M. Kurzawa, J. Thermal Anal., 31 (1986) 531.
7 J. Walczak and E. Filipek, Thermochim. Acta, 150 (1989) 125.
8 M. Kurzawa, J. Mater. Sci. Lett., 11 (1992) 996.
9 J. Walczak, E. Filipek and P. Tabero, Thermochim. Acta, 206 (1992) 279.
10 A. F. Wells, Structural Inorganic Chemistry, Oxford University Press, 1984, pp. 504–506.
11 S. Westman and A. Magneli, Acta Chem. Scand., 12 (1958) 363.
12 E. Salje, R. Gehlig and K. Viswanathan, J. Solid State Chem., 25 (1978) 239.
13 L. Kihlborg, Acta Chem. Scand., 21 (1967) 2495.
14 A. Bielanski, K. Dyrek, J. Pozniczek and E. Wenda, Bull. Acad. Polon. Sci. Ser. Sci. Chim., 19 (1971) 507.
15 R. C. T. Slade, A. Ramanan, J. M. Nicol and C. Ritter, Mater. Res. Bull., 23 (1988) 647.
16 T. Hirata and Y. Zhu, J. Phys. Condens. Matter, 4 (1992) 7377.
17 J. Darriet, J. Galy and P. Hagenmuller, J. Solid State Chem., 3 (1971) 596.
18 E. Burzo, L. Stanescu and D. Ungur, Solid State Commun., 18 (1976) 537.
19 H.-Y. Chen, Mater. Res. Bull., 14 (1979) 1583.
20 J. Senegas and J. Galy, J. Solid State Chem., 10 (1974) 5.
21 J. Walczak, I. Rychlowska-Himmel and P. Tabero, J. Mater. Sci., 27 (1992) 3680.
22 W. T. A. Harrison, U. Chowdhry, C. J. Machiels, A. W. Sleight and A. K. Cheetham, J. Solid State Chem., 60 (1985) 101.
23 M. Kurzawa and A. Blonska-Tabero, J. Therm. Anal. Cal., 77 (2004) 65.
24 M. Kurzawa and A. Blonska-Tabero, J. Therm. Anal. Cal., 77 (2004) 17.
25 L. Wachowski and M. Hofman, J. Therm. Anal. Cal., 83 (2006) 379.
26 A. Skaropoulou, G. Kahali and S. Tsivilis, J. Therm. Anal. Cal., 84 (2006) 135.
27 E. T. Stepkowska, J. M. Blanes, A. Justo, M. A. Aviles and J. L. Perez-Rodriguez, J. Therm. Anal. Cal., 80 (2005) 193.
28 Powder Diffraction File International Centre for Diffraction Data, Swarthmore, USA 1989, File Nos: 34-527, 35-609, 48-741, 70-2024, 77-2418, 83-951, 89-599.
29 E. J. Baran and I. L. Botto, Monatsh. Chem., 108 (1977) 311.
30 D. J. Roncaglia, I. L. Botto and E. J. Baran, J. Solid State Chem., 62 (1986) 11.
31 J. Preudhomme and P. Tarte, Spectrochim. Acta, 27A (1971) 961, 1817.

DOI: 10.1007/s10973-006-8047-7